

L. Romaka<sup>1</sup>, K. Miliyanchuk<sup>1</sup>, V.V. Romaka<sup>2</sup>, L. Havela<sup>3</sup>, Yu. Stadnyk<sup>1</sup>

## Structural studies and magnetism of Dy<sub>6</sub>Ni<sub>2.43</sub>Sn<sub>0.5</sub> stannide

<sup>1</sup>Department of Inorganic Chemistry, Ivan Franko National University of Lviv, Lviv, Ukraine, [lyubov.romaka@gmail.com](mailto:lyubov.romaka@gmail.com)

<sup>2</sup>Institute for Solid State Research, IFW-Dresden, Dresden, Germany

<sup>3</sup>Department of Condensed Matter Physics, Charles University, Prague 2, The Czech Republic

Intermetallic compound Dy<sub>6</sub>Ni<sub>2.43</sub>Sn<sub>0.5</sub> was prepared by arc melting and annealing at 873 K. It was characterized by X-ray powder diffraction, differential thermal analysis, and electron probe microanalysis. The crystal structure of low temperature Dy<sub>6</sub>Ni<sub>2.43</sub>Sn<sub>0.5</sub> phase belongs to the orthorhombic Ho<sub>6</sub>Co<sub>2</sub>Ga structure type (space group *Immm*, *a* = 0.93116(1) nm, *b* = 0.94993(1) nm, *c* = 0.98947(1) nm). Crystal structure refinements showed the deviation from the ideal 6:2:1 stoichiometry corresponding to the formula Dy<sub>6</sub>Ni<sub>2.43</sub>Sn<sub>0.5</sub>. It exhibits a sequence of magnetic phase transitions; antiferromagnetic ordering sets in at 60 K, while further order-order magnetic phase transitions take place at lower temperatures.

**Keywords:** Intermetallics; Crystal structure; Magnetic properties; Heat capacity.

Received 16 January 2023; Accepted 26 April 2023.

## Introduction

The search of new intermetallics with useful magnetic properties has brought lot of attention to compounds containing rare earths (*R*), *d*-metals (*M*), and *p*-elements (*X*) such as Si, Ga, Ge, Sn, In, Pb. In the *R*-rich region of the *R*-*M*-*X* ternary systems (*M* = Co, Ni; *X* = Ga, In, Sn, Pb) two series of isotypic compounds *R*<sub>12</sub>*M*<sub>6</sub>*X* (cubic Sm<sub>12</sub>Ni<sub>6</sub>In-type) and *R*<sub>6</sub>*M*<sub>2</sub>*X* (orthorhombic Ho<sub>6</sub>Co<sub>2</sub>Ga-type) were identified and studied previously [1-8]. Both types of crystal structures are characterized by the antiprismatic-tetragonal coordination of the smaller atoms (Co, Ni) and by significant shortening of interatomic distances between rare earths and *d*-elements and between *M* atoms. The relationship between Sm<sub>12</sub>Ni<sub>6</sub>In and Ho<sub>6</sub>Co<sub>2</sub>Ga structure types is described in Ref. [8]. In the Ho<sub>6</sub>Co<sub>2</sub>Ga structure, the rare earth atoms form metal bonded framework yielding several types of high coordination polyhedra encapsulating the atoms of the transition metals and *X* elements [4]. Depending on the ratio of the size of the atoms *M* and *X*, the tendency for disorder in particular crystallographic sites is observed in these structures. For example, the compounds Tb<sub>6</sub>Co<sub>2.35</sub>Sn<sub>0.65</sub> [9], Ho<sub>6</sub>Co<sub>2.135</sub>In<sub>0.865</sub> [6], Er<sub>6</sub>Co<sub>2.19</sub>In<sub>0.81</sub> [10], and *R*<sub>6</sub>*M*<sub>2+x</sub>Pb<sub>1-x</sub> (*M* = Co, Ni) [8] are characterized

by statistical mixture of *M* and *X* atoms in the 2*a* site, while in the original Ho<sub>6</sub>Co<sub>2</sub>Ga structure type it is occupied exclusively by Ga atoms. In Dy<sub>6</sub>Co<sub>2.5</sub>Sn<sub>0.5</sub>, the Co atoms occupy three crystallographic sites, and only 2*c* position is occupied by the Sn atoms [11]. Study of isotypic compounds with bismuth [12] showed that unlike the Ho<sub>6</sub>Co<sub>2</sub>Ga prototype, the 2*a* position is occupied by Co atoms and authors propose the formula *R*<sub>12</sub>Co<sub>5</sub>Bi (equal to *R*<sub>6</sub>Co<sub>2.5</sub>Bi<sub>0.5</sub>) which reflects the occupancy of crystallographic positions in the structure.

Taking into account that the complex magnetic behavior arises from the connection of *f*- and *d*-electrons in rare-earth intermetallics with transition elements, the properties of stannides *R*<sub>12</sub>Ni<sub>6</sub>Sn and *R*<sub>6</sub>*M*<sub>2</sub>Sn were explored. A study of magnetic properties revealed that the *R*<sub>12</sub>Ni<sub>6</sub>Sn intermetallics exhibit ferromagnetic ordering for Gd and Tb compounds with *T*<sub>C</sub> = 85 K and 95 K, respectively [1]. The temperature dependencies of the magnetic susceptibility measured earlier in the range 78-293 K for *R*<sub>6</sub>Ni<sub>2</sub>Sn compounds (*R* = Tb, Dy, Er, and Tm) showed that they obey the Curie-Weiss law with effective magnetic moments close to free *R*<sup>3+</sup> ion values [5, 7].

The isotypic stannide Er<sub>6</sub>Ni<sub>2</sub>Sn has been investigated as potential material for the lower temperature stage of Gifford-McMahon cryocooler [13]. Refs. [14,15]

suggested, based on specific-heat data and magnetic measurements of Er<sub>6</sub>Ni<sub>2</sub>Sn giving estimates of isothermal entropy change and magnetocaloric effect, that this compound can serve as material for cryogenic devices. Neutron diffraction study of Er<sub>6</sub>Ni<sub>2</sub>Sn showed a complex non-collinear commensurate antiferromagnetic structure [16], in which the magnetic moment values of Er atoms are significantly reduced.

The present work aims to determine structure characteristics and magnetic properties of Dy<sub>6</sub>Ni<sub>2.43</sub>Sn<sub>0.5</sub>. In addition, magnetic behaviour of the binary Dy<sub>5</sub>Sn<sub>3</sub> is presented.

## I. Experimental details

Polycrystalline samples for investigation were prepared by direct arc melting of the constituent metals (dysprosium, purity 99.9 wt.%; nickel, purity 99.99 wt.%; tin, purity 99.999 wt.%) under purified argon atmosphere (Ti as a getter) in a water-cooled copper crucible. Weight losses of the initial batch did not exceed 1 wt. %. Two pieces of the alloys were annealed separately in the evacuated quartz ampoules at  $T = 873$  K and  $T = 1073$  K for 720 hours and then quenched in cold water. The synthesized and annealed samples are stable under ambient conditions. The chemical composition of the prepared samples was examined by Scanning Electron Microscopy using JEOL-840A scanning microscope.

X-ray powder diffraction data were collected using STOE STADI P powder diffractometer (Cu  $K\alpha_1$  radiation, angular range for data collection  $6.000 \leq 2\theta \leq 110.625/0.015$ ). FullProf Suite program package [17] was used for the determination of the crystal structure parameters.

Differential thermal analysis (DTA) was used to check the temperature range of the stability of the compound (LINSEIS STA PT 1600 device, argon atmosphere). Sample was heated up to 1173 K, at a rate of 10 K/min. The weight losses during heating (TG) were less than 0.2%.

The magnetic susceptibility was measured in external magnetic fields up to 9 T in the temperature range from 2 K to 300 K using a Quantum Design PPMS extraction magnetometer. The grains of the sample were fixed in random orientation preventing rotation of individual grains under the influence of a magnetic field. The specific heat measurements were performed on a bulk sample in the same temperature range using a Quantum Design PPMS microcalorimetry setup.

The magnetic behavior of the Dy<sub>5</sub>Sn<sub>3</sub> compound was measured using an extraction method in the magnetic fields up to 10 T in the temperature range 2 K to 300 K.

## II. Results and discussion

### 2.1. Formation of compounds and crystal structure refinement

Taking into account the literature data and general stoichiometry 6:2:1 for the  $R_6Ni_2Sn$  series, a polycrystalline sample with nominal composition Dy<sub>67</sub>Ni<sub>22</sub>Sn<sub>11</sub> was prepared. X-ray phase analysis of the

sample showed the presence of the main phase Dy<sub>6</sub>Ni<sub>2</sub>Sn with the Ho<sub>6</sub>Co<sub>2</sub>Ga structure type and a small amount of additional binary phase Dy<sub>5</sub>Sn<sub>3</sub> (Mn<sub>5</sub>Si<sub>3</sub> structure type,  $a = 0.88863(1)$ ,  $c = 0.64873(1)$  nm). According to the electron probe microanalysis (EPMA) data, the determined composition of the main phase is Dy<sub>66.62</sub>Ni<sub>27.67</sub>Sn<sub>5.71</sub>, meaning lower Sn concentration in comparison with the ideal 6:2:1 stoichiometry. As the next step, we prepared a new sample with the nominal composition Dy<sub>66</sub>Ni<sub>28</sub>Sn<sub>6</sub>. In order to synthesize a single-phase sample we used two different temperatures of annealing, namely 873 and 1073 K. The phase analysis of the sample annealed at 873 K proved the existence of orthorhombic phase with the Ho<sub>6</sub>Co<sub>2</sub>Ga structure type, while a phase with the cubic Sm<sub>12</sub>Ni<sub>6</sub>In structure type was identified in the sample annealed at 1073 K. To confirm a polymorphic transition we have studied the sample by the differential thermal analysis. The DTA curve measured in the heating and cooling regimes is shown in Fig. 1. Two thermal peaks are more visible on the cooling curve at 1098.5 K and 1015.3 K, respectively, which can be associated with the formation of the cubic phase and next polymorphic transition to the orthorhombic one. Thus, we can say that orthorhombic phase is stable up to  $\approx 1015$  K.

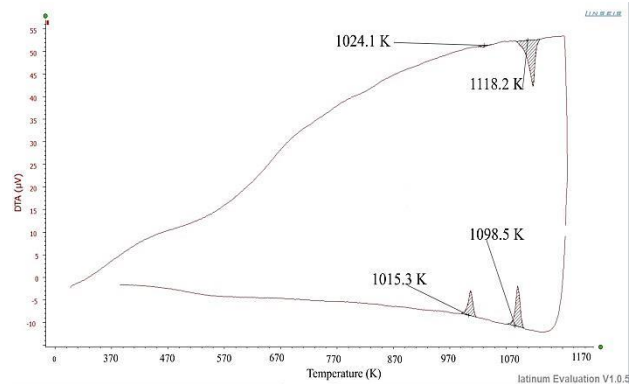


Fig. 1. DTA plot for Dy<sub>66</sub>Ni<sub>28</sub>Sn<sub>6</sub> sample.

Analysis of X-ray powder diffraction pattern of the Dy<sub>66</sub>Ni<sub>28</sub>Sn<sub>6</sub> sample annealed at  $T = 870$  K showed the presence of a single phase with orthorhombic Ho<sub>6</sub>Co<sub>2</sub>Ga-type (space group  $Immm$ ,  $a = 0.93116(1)$  nm,  $b = 0.94993(1)$  nm,  $c = 0.98947(4)$  nm). Refined atomic coordinates and displacement parameters for Ho<sub>6</sub>Co<sub>2</sub>Ga-type phase are listed in Table 1. The refinement of the site occupancies showed that in this structure Ni atoms fully occupy the 4j position and both 4g and 2a positions for Ni atoms are occupied partially (Table 1). Thus, the chemical formula should be written as Dy<sub>6</sub>Ni<sub>2.43</sub>Sn<sub>0.5</sub>, what is in a good agreement with EPMA data (Dy<sub>66.62</sub>Ni<sub>27.67</sub>Sn<sub>5.71</sub>). Obtained stoichiometry is close to the previously studied Tb<sub>6</sub>Co<sub>2.35</sub>Sn<sub>0.65</sub> [9] and  $R_6M_{2+x}Pb(In)_{1-x}$  ( $M = Co, Ni$ ) [6,8,10] compounds, which are characterized by a lower concentration of the p-element compared to the ordered Ho<sub>6</sub>Co<sub>2</sub>Ga-type phase.

Crystal chemical analysis of the stannide Dy<sub>6</sub>Ni<sub>2.43</sub>Sn<sub>0.5</sub> showed that this structure can be presented as a framework of Dy atoms forming prismatic and icosahedral polyhedra filled with the smaller Ni and Sn atoms (Fig. 2) The analysis of the interatomic distances in the Dy<sub>6</sub>Ni<sub>2.43</sub>Sn<sub>0.5</sub> structure showed a significant variations

**Table 1.**Atomic coordinates and isotropic displacement parameters for the  $\text{Dy}_6\text{Ni}_{2.43}\text{Sn}_{0.5}$  compound $(R_{\text{Bragg}} = 0.039, R_p = 0.011, R_{\text{wp}} = 0.015)$ 

Atom	Wyckoff position	$x/a$	$y/b$	$z/c$	$*B_{\text{iso}} \cdot 10^2$ (nm <sup>2</sup> )	Occupancy
Dy1	8n	0.2924(2)	0.1821(2)	0	1.17(8)	1
Dy2	8m	0.3030(2)	0	0.3233(1)	0.49(8)	1
Dy3	8l	0	0.1903(2)	0.2146(2)	0.84(8)	1
Ni1	4j	1/2	0	0.1233(6)	1.72(2)	1
Ni2	4g	0	0.3633(7)	0	1.57(6)	0.95(1)
Ni3	2a	0	0	0	1.62(1)	0.96(1)
Sn	2c	1/2	1/2	0	0.88(1)	1

of the sum of the corresponding atomic radii ( $r_a(\text{Dy}) = 0.177$  nm,  $r_a(\text{Ni}) = 0.125$  nm): for shorter Dy-Ni distances Dy1-Ni1 – 0.2849 nm; Dy2-Ni2 – 0.2847 nm; Dy3-Ni2 – 0.2821 nm and Ni1-Ni1 distance 0.2440 nm. The shortening in interatomic distances in  $\text{Dy}_6\text{Ni}_{2.43}\text{Sn}_{0.5}$  is similar to the shortening in the prototype  $\text{Ho}_6\text{Co}_2\text{Ga}$  [4] and in other isotopic intermetallics with Sn or Pb [8, 9].

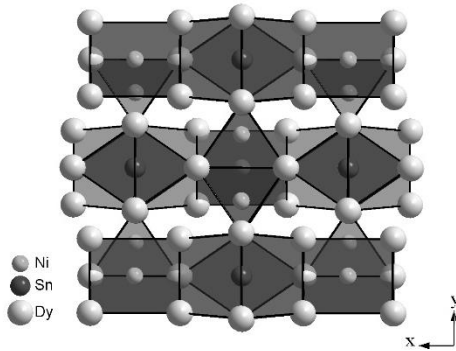


**Fig. 2.** Atomic columns in  $\text{Dy}_6\text{Ni}_{2.43}\text{Sn}_{0.5}$  structure formed by Dy atoms. The smaller Ni and Sn atoms are inside prismatic and icosahedral voids.

It should be pointed out that the crystal structure of  $\text{Dy}_6\text{Ni}_{2.43}\text{Sn}_{0.5}$  can be derived from the  $\text{WAl}_{12}$  structure type by an insertion of Ni and Sn atoms into binary  $\text{WAl}_{12}$  [7]. Both compounds are characterized by similar 3D-framework structure built by Dy and Al atoms, respectively (Fig. 3).

The analysis of the structures  $\text{Ho}_6\text{Co}_2\text{Ga}$  [4] and the isotopic  $R_6M_{2+x}X_{1-x}$  intermetallics ( $M = \text{Co}, \text{Ni}$  and  $X = \text{Ga},$

In, Sn, Pb, and Bi) [5-12] illustrated the role of the size of the  $X$  element in structural disorder. The  $\text{Ho}_6\text{Co}_2\text{Ga}$  structure is completely ordered, small Ga atoms occupy two crystallographic sites  $2c$  and  $2a$  fully. Crystal structures of the related compounds with larger  $X$  atoms show that the crystallographic position  $2a$ , occupied only by Ga atoms in  $\text{Ho}_6\text{Co}_2\text{Ga}$ -type, is strongly susceptible to accommodate statistical mixtures with  $d$ -metals, what results in a deviation from the ideal stoichiometry 6:2:1. This fact was observed for the compounds  $\text{Tb}_6\text{Co}_{2.35}\text{Sn}_{0.65}$ ,  $\text{Ho}_6\text{Co}_{2.135}\text{In}_{0.865}$ ,  $\text{Er}_6\text{Co}_{2.19}\text{In}_{0.81}$ ,  $R_6M_{2+x}\text{Pb}(\text{Bi})_{1-x}$  [6, 8-12], and finally for  $\text{Dy}_6\text{Ni}_{2.43}\text{Sn}_{0.5}$ .

## 2.2. Magnetic and heat capacity measurements

For the  $\text{Dy}_{67}\text{Ni}_{22}\text{Sn}_{11}$  sample we performed magnetic susceptibility measurements in magnetic field of 0.05 T, 2 T, and 4 T in the temperature range 2-300 K. The field dependence of magnetization was measured in magnetic fields up to 9 T for temperatures  $T = 2, 20,$  and 40 K. Fig. 4 shows that the high temperature Curie-Weiss behavior extends down only to 60-70 K and below this temperature the values of  $\chi(T)$  become field dependent. In the paramagnetic state the temperature dependence of the inverse magnetic susceptibility  $\chi^{-1}(T)$  is well described by the Curie-Weiss law with the value of effective moment  $10.60 \mu_B/\text{Dy}$ , *i.e.* close to the value for free ion  $\text{Dy}^{3+}$  ( $10.65 \mu_B$ ) (Fig. 5). The paramagnetic Curie temperature  $\theta_p = 26$  K is lower than the transition temperature but still positive, which indicates predominant ferromagnetic interactions. Temperature behavior of the magnetic susceptibility exhibits a kink, pointing to an antiferromagnetic ordering below about

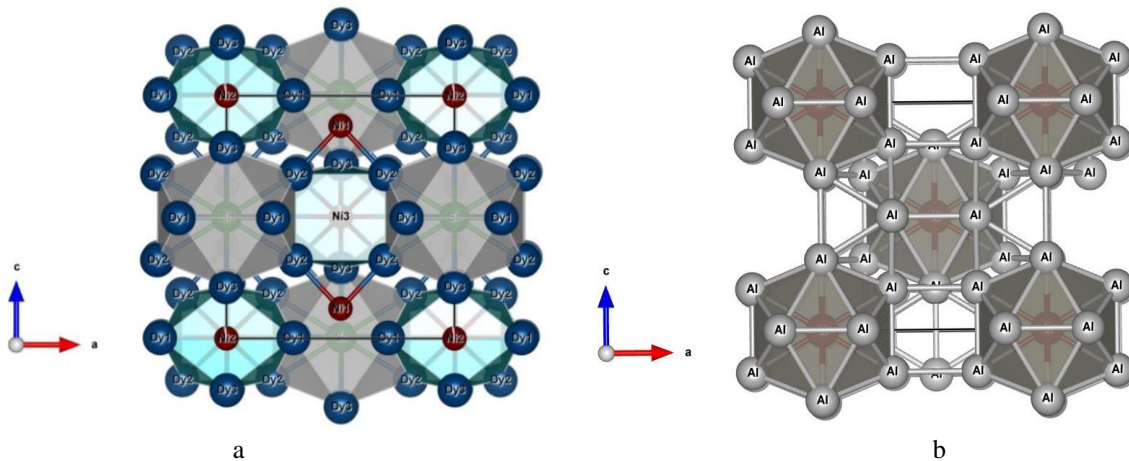


**Fig. 3.** Model of  $\text{Dy}_6\text{Ni}_{2.43}\text{Sn}_{0.5}$  (a) and  $\text{WAl}_{12}$  (b) structures.

60 K (see Fig. 4). However,  $\chi(T)$  still increases below this temperature (at least in low magnetic fields) and another kink is visible at  $T = 27$  K, which may suggest presence of a magnetic phase transition of the order-order type. A smaller anomaly see particularly for the 2 T data can be distinguished at 19 K. The  $\chi(T)$  measurement in very low magnetic field (0.05 T) reveals a small ferromagnetic component developing below  $T = 60$  K. As the size of the increment in the inset of Fig. 4 is  $\approx 6 \times 10^{-5} \text{ m}^3/\text{mol f.u.}$ , i.e.  $< 0.5 \mu_B/\text{f.u.}$ , it means less than  $0.1 \mu_B/\text{Dy}$ . Hence we most likely encounter a defected antiferromagnetic structure with incomplete cancelation of sublattices, related most likely to the statistical occupancy of several crystallographic sites. Although the magnetism has been related to Dy only and no Ni moments are anticipated, the defected Dy environment brings randomness into the RKKY interaction, yielding certain features of magnetic glass, as magnetic history phenomena in antiferromagnet. This suggestion is corroborated by the fact that there is residual magnetization of  $2 \mu_B/\text{f.u.}$  when returning to zero field from a high field state in  $\mu_0 H = 9$  T at  $T = 2$  K (see Fig. 6).

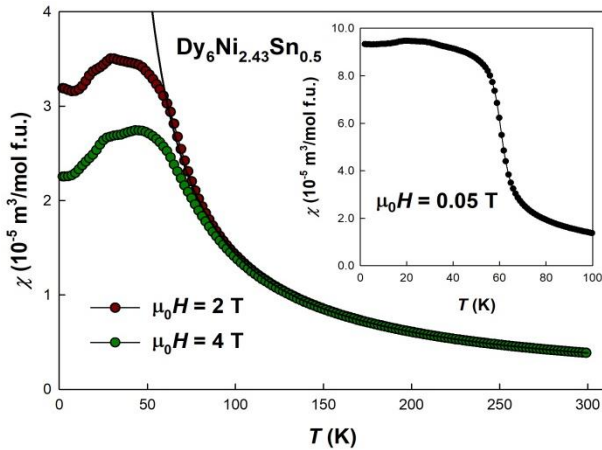


**Fig. 4.** Temperature dependences of the magnetic susceptibility  $\chi(T)$  of Dy<sub>6</sub>Ni<sub>2.43</sub>Sn<sub>0.5</sub> in various magnetic fields. Detail of low-field data are shown in the inset.

The magnetization curve measured at  $T = 2$  K (Fig. 6) exhibits a metamagnetic process starting at  $\mu_0 H \approx 3$  T, which brings the total magnetization to the level of  $25\text{--}30 \mu_B/\text{f.u.}$  It is still only a half of the theoretical total magnetization of  $60 \mu_B/\text{f.u.}$  The related broad hysteresis becomes narrower but it is still observed at 20 K, shifting the metamagnetic transition to lower fields, while both hysteresis and metamagnetic transition disappear at 40 K. The total magnetization achieved can be naturally affected by anisotropy, the type and strength remain unknown. For example, only 50% of total magnetization is measured if a strongly anisotropic material with uniaxial anisotropy is measured in the form of randomly oriented polycrystal. Therefore it is also impossible to determine with certainty whether the metamagnetism is of the spin-flip or spin-flop type. Even in the first case, the distribution of orientation of individual grains with respect to the field direction can cause a spreading of the transition over a large field range.

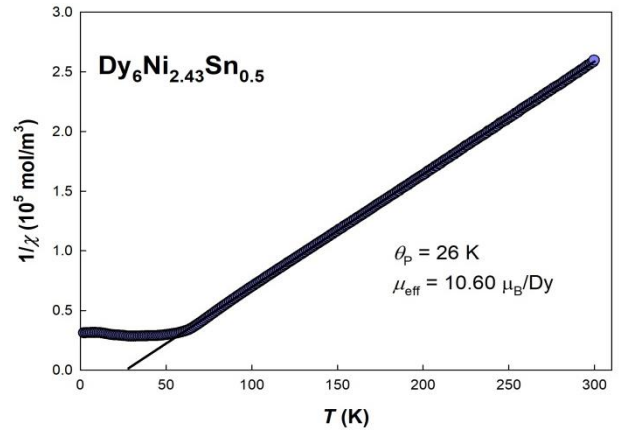


**Fig. 5.** Temperature dependence of the inverse magnetic susceptibility of the Dy<sub>6</sub>Ni<sub>2.43</sub>Sn<sub>0.5</sub> compound ( $\mu_0 H = 2$  T).

Complementary information can be obtained from the temperature dependence of specific heat at constant pressure,  $C_p(T)$ . It exhibits a clear phase transition at  $T = 62$  K, which remains practically unchanged in magnetic field of 2 T (Fig. 7).

External magnetic field of 9 T, *i.e.* exceeding the critical metamagnetic field, removes the magnetic phase transition and the related entropy is displaced to higher temperatures as in ferromagnets. Therefore we can assume that the state above the metamagnetic transition corresponds to field-aligned paramagnetic state, however not necessarily with full collinearity of magnetic moments. The slope of  $M(H)$  in 9 T indicates that the alignment process would continue even to much higher fields. At low temperatures one can use the  $C_p/T(T^2)$  plot to determine the Sommerfeld coefficient of electronic specific heat  $\gamma$  as the intercept of extrapolated line with the vertical axis (see inset). For Dy<sub>6</sub>Ni<sub>2.43</sub>Sn<sub>0.5</sub> we can make only a very approximate estimate yielding  $\gamma \approx 200 \text{ mJ/mol f.u. K}^2$ . The linear part is actually short, limited from below probably by the nuclear heat capacity component of Dy [18].

As presence of a small amount of Dy<sub>5</sub>Sn<sub>3</sub> in the sample has been indicated, a question is whether some of the anomalies observed can be associated with such spurious phase. Therefore we prepared Dy<sub>5</sub>Sn<sub>3</sub> sample, annealed at  $T = 873$  K, and its magnetic behavior determined. According to X-ray analysis, Dy<sub>5</sub>Sn<sub>3</sub> crystallizes in the Mn<sub>5</sub>Si<sub>3</sub> structure type (space group  $P6_3/mcm$ ) with refined lattice parameters  $a = 0.88633(1)$ ,  $c = 0.64873(1)$  nm. The maximum in the temperature dependence of the magnetic susceptibility in the temperature range 2-100 K indicates an antiferromagnetic ordering at  $T_N = 20$  K (Fig. 8,a). Analysis of the temperature dependence of the inverse magnetic susceptibility showed that the paramagnetic Curie temperature is  $\theta_p = 14$  K, calculated effective moment  $10.71 \mu_B/\text{Dy}$  is close to Dy<sup>3+</sup>. The field dependencies of the magnetization are displayed in Fig. 8,b. At low temperatures they reveal rather fast initial increase and a weak tendency to saturation in fields exceeding 5-6 T. It can be interpreted as canting of Dy moments starting from low fields already. Therefore the antiferromagnetic transition is eliminated in the field of 1 T. Hence Dy<sub>5</sub>Sn<sub>3</sub> cannot be taken responsible low-temperature anomalies seen in  $\chi(T)$  for Dy<sub>6</sub>Ni<sub>2.43</sub>Sn<sub>0.5</sub> in the field of 2 or 4 T.

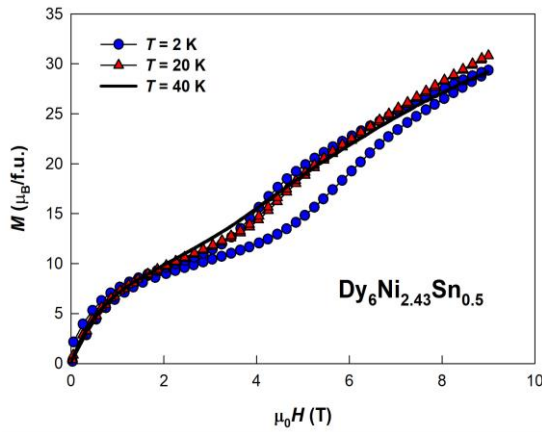


**Fig. 6.** Field dependence of magnetization of  $\text{Dy}_6\text{Ni}_{2.43}\text{Sn}_{0.5}$  at various temperatures with field swept up and down.

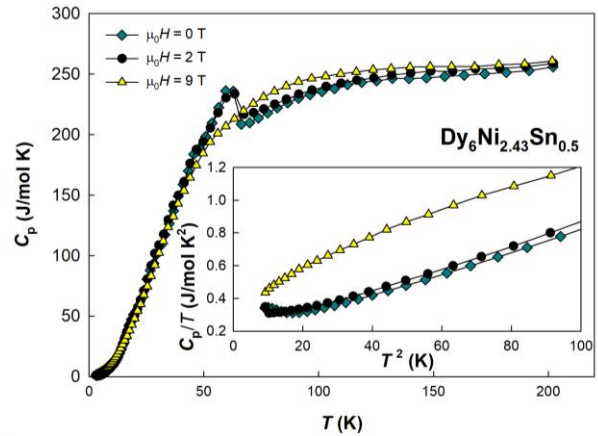


**Fig. 7.** Temperature dependence of the specific heat of  $\text{Dy}_6\text{Ni}_{2.43}\text{Sn}_{0.5}$ .

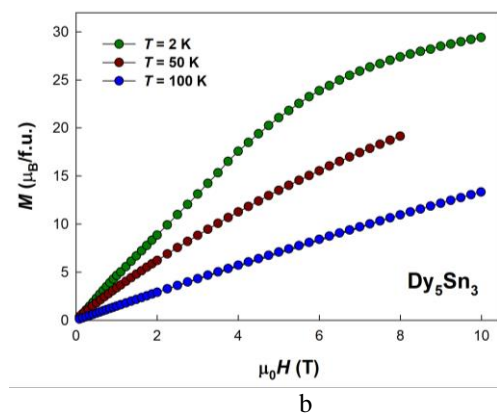
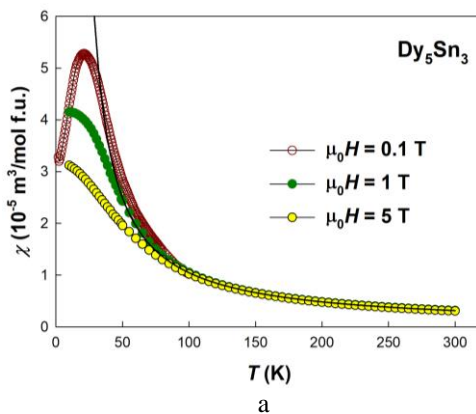


**Fig. 8.** Temperature dependence of the magnetic susceptibility of  $\text{Dy}_5\text{Sn}_3$  at various magnetic fields (a); magnetization vs magnetic field at different temperatures (b).

Considerable anomalies concerning the magnetic ordering of impurity phase  $\text{Dy}_5\text{Sn}_3$  were not observed in the temperature dependence of magnetic susceptibility of  $\text{Dy}_6\text{Ni}_{2.43}\text{Sn}_{0.5}$ . Taking into account this result we can rule out contribution of impurity phase  $\text{Dy}_5\text{Sn}_3$  in the magnetism of the  $\text{Dy}_6\text{Ni}_{2.43}\text{Sn}_{0.5}$  stannide.

## Conclusions

Structure refinements of the  $\text{Dy}_6\text{Ni}_{2.43}\text{Sn}_{0.5}$  compound confirmed that this compound belongs to the orthorhombic  $\text{Ho}_6\text{Co}_2\text{Ga}$  structure type but contrary to the prototype  $\text{Ho}_6\text{Co}_2\text{Ga}$  compound a significant deviation from the 6:2:1 stoichiometry has been observed. This deviation is caused by the exclusive presence of Ni atoms at the 2a site and a partial occupation of the 4g and 2a sites by Ni atoms. The phase situation is, however, affected by annealing.

The results of the magnetic and heat capacity measurements indicated a magnetic transition at 60 K connected with antiferromagnetic ordering. Further order-order phase transitions have been observed at lower

temperatures. The calculated effective magnetic moments in paramagnetic state is closed to the value for free ion  $\text{Dy}^{3+}$ , indicating a main role of rare earth in the magnetism of  $\text{Dy}_6\text{Ni}_{2.43}\text{Sn}_{0.5}$ . Statistical occupation of several Ni sites yields a glassy behavior and magnetic history phenomena.

## Acknowledgements

We would like to acknowledge financial support of the Ministry of Education and Science of Ukraine under Grant No. 0121U109766. We also thank Prof. O. Isnard for assistance with collecting part of the magnetic data.

**Romaka Lyubov** – Ph.D., Senior Researcher, Ivan Franko National University of Lviv;  
**Miliyanchuk Khrystyna** – Ph.D., Senior Researcher, Ivan Franko National University of Lviv;  
**Romaka Vitaliy** – D.Sc., Doctor of material science, Institute for Solid State Research, Dresden, Germany;  
**Havela Ladislav** – CSc., RNDr, Senior Researcher, Charles University, Prague, Czech Republic;  
**Stadnyk Yuriy** – Ph.D., Senior Researcher, Ivan Franko National University of Lviv.

[1] L. Romaka, O. Senkovska, D. Fruchart, D. Gignoux, Gignoux, *Crystal structure and magnetic properties of new rare earth  $R_{12}\text{Ni}_6\text{Sn}$  compounds*, J. Magn. Mater., 242-245, 854 (2002); [https://doi.org/10.1016/S0304-8853\(01\)01342-7](https://doi.org/10.1016/S0304-8853(01)01342-7).

- [2] Ya.M. Kalychak, *Composition and crystal structure of rare-earths-Co-In compounds*, J. Alloys Compd., 291, 80 (1999); [https://doi.org/10.1016/S0925-8388\(99\)00290-X](https://doi.org/10.1016/S0925-8388(99)00290-X).
- [3] L.D. Gulay, Ya.M. Kalychak, M. Wolcyrz, K. Lukaszewicz, *Crystal structure of R<sub>12</sub>Ni<sub>6</sub>Pb (R = Y, Sm, Gd, Tb, Dy, Ho, Er, Tm, Lu) compounds*, J. Alloys Compd., 311, 238 (2000); [https://doi.org/10.1016/S0925-8388\(00\)01115-4](https://doi.org/10.1016/S0925-8388(00)01115-4).
- [4] R.E. Gladyshevskii, Yu.N. Gryn', Ya.P. Yarmolyuk, *The crystal structure of R<sub>6</sub>GaCo<sub>2</sub> compounds (R = Y, Tb, Dy, Ho, Er, Tm, Lu)*, Dopov. Akad. Nauk Ukr. RSR A2, 67 (1983).
- [5] O.M. Sichevich, L.P. Komarovskaja, Yu.N. Grin, Ya.P. Yarmolyuk, R.V. Skolozdra, *Crystal structure and magnetic properties of R<sub>6</sub>Ga[Co,Ni]<sub>2</sub> and R<sub>6</sub>SnNi<sub>2</sub> compounds (R-rare earths)*, Ukr. J. Phys., 29, 1342 (1984).
- [6] J.M. Kalychak, V.I. Zaremba, P.Y. Zavalij, *Crystal structure of holmium cobalt indium (6/2/1) Ho<sub>6</sub>Co<sub>2+x</sub>In<sub>1-x</sub>, x = 0.135*, Z. Kristallogr. 208, 380 (1993).
- [7] R.V. Skolozdra, in: K.A. Gschneidner, Jr., L.Eyring (Eds.), *Handbook on the Physics and Chemistry of Rare-Earths*, Vol. 24, North-Holland, Amsterdam, 1997, chapt. 164.
- [8] L.D. Gulay, M. Wolcyrz, *Crystal structure of R<sub>6</sub>Co<sub>2+x</sub>Pb<sub>1-y</sub> (R = Y, Gd, Tb, Dy, Ho, Er, Tm, Lu) and R<sub>6</sub>Ni<sub>2+x</sub>Pb<sub>1-y</sub> (R = Tb, Dy, Ho, Er, Tm, Lu) compounds*, J. Alloys Compd., 315, 164 (2001); [https://doi.org/10.1016/S0925-8388\(00\)01281-0](https://doi.org/10.1016/S0925-8388(00)01281-0).
- [9] A.V. Kolomiets, Ya. Mudryk, Yu. Stadnyk, V. Sechovsky, *Crystal structure and magnetic properties of Tb<sub>6</sub>Co<sub>2.35</sub>Sn<sub>0.65</sub>*, J. Alloys Compd., 333, 34 (2002); [https://doi.org/10.1016/S0925-8388\(01\)01715-7](https://doi.org/10.1016/S0925-8388(01)01715-7).
- [10] V.I. Zaremba, Y.M. Kalychak, M.V. Dzevenko, U.C. Rodewald, R.D. Hoffmann, R. Pöttgen, *Syntheses and structure of Er<sub>6</sub>Co<sub>2.19(1)</sub>In<sub>0.81(1)</sub>*, Monatsh. Chem., 138, 101 (2007); <https://doi.org/10.1007/s00706-006-0572-3>.
- [11] A.V. Morozkin, R. Nirmala, S.K. Malik, *Magnetic and magnetocaloric properties of Ho<sub>6</sub>Co<sub>2</sub>Ga-type Dy<sub>6</sub>Co<sub>2.5</sub>Sn<sub>2.5</sub> compound*, J. Magn. Magn. Mater., 378, 174 (2015); <https://doi.org/10.1016/j.jmmm.2014.11.011>.
- [12] A.V. Tkachuk, A. Mar, *Structure and physical properties of ternary rare-earth cobalt bismuth intermetallics (RE)<sub>12</sub>Co<sub>5</sub>Bi (RE = Y, Gd, Tb, Dy, Ho, Er, Tm)*, Inorg. Chem., 44(7), 2272 (2005); <https://doi.org/10.1021/ic048195p>.
- [13] K.A. Gschneidner, V.K. Pecharsky, M. Gailloux, in: R.G. Ross Jr. (Ed.), *Cryocoolers 8*, Plenum Press, New-York, 1995.
- [14] O. Syshchenko, Yu. Stadnyk, L. Romaka, Ya. Mudryk, R.V. Dremov, V. Sechovsky, *Magnetic and transport properties of Er<sub>6</sub>Ni<sub>2</sub>Sn*, J. Alloys Compd., 319, 14 (2001); [https://doi.org/10.1016/S0925-8388\(01\)00877-5](https://doi.org/10.1016/S0925-8388(01)00877-5).
- [15] D. Vasylyev, O. Syshchenko, V. Sechovsky, J. Sebek, Yu. Stadnyk, Ya. Mudryk, L. Romaka, *Magnetocaloric effect in Er<sub>6</sub>Ni<sub>2</sub>Sn*, Czech. J. Phys., 52, A205 (2002); <https://doi.org/10.1007/s10582-002-0049-5>.
- [16] K. Prokes, V. Sechovsky, O. Syshchenko, *Magnetic structure of Er<sub>6</sub>Ni<sub>2</sub>Sn*, J. Alloys Compd., 48-53, 467 (2009); <https://doi.org/10.1016/j.jallcom.2007.12.022>.
- [17] T. Roisnel, J. Rodriguez-Carvajal, *WinPLOTR: a Windows tool for powder diffraction patterns analysis*, Mater. Sci. Forum, 378-381, 118 (2001). <https://doi.org/10.4028/www.scientific.net/MSF.378-381.118>
- [18] O.V. Lounasmaa, R. A. Guenther, *Specific heat of dysprosium metal between 0.4 and 4°K*, Phys. Rev., 126, 1357 (1962); <https://doi.org/10.1103/PhysRev.126.1357>

Л. Ромака<sup>1</sup>, Х. Міліянчук<sup>1</sup>, В.В. Ромака<sup>2</sup>, Л. Гавела<sup>3</sup>, Ю. Стадник<sup>1</sup>

## Структурні дослідження і магнетизм станіду Dy<sub>6</sub>Ni<sub>2.43</sub>Sn<sub>0.5</sub>

<sup>1</sup>Львівський національний університет ім. І.Франка, Львів, Україна, [lyubov.romaka@gmail.com](mailto:lyubov.romaka@gmail.com)

<sup>2</sup>Інститут досліджень твердого тіла, IFW-Дрезден, Дрезден, Німеччина

<sup>3</sup>Кафедра фізики твердого тіла, Карлів університет, Прага 2, Чехія

Інтерметалід Dy<sub>6</sub>Ni<sub>2.43</sub>Sn<sub>0.5</sub> отриманий методом електродугового плавлення і гомогенізуючого відпалювання за температури 873 К. Сполука досліджена методами рентгенівської дифрактометрії, диференціального термічного аналізу і енергодисперсійної спектроскопії. Кристалічна структура низькотемпературної фази Dy<sub>6</sub>Ni<sub>2.43</sub>Sn<sub>0.5</sub> належить до орторомбічного структурного типу Ho<sub>6</sub>Co<sub>2</sub>Ga (просторова група *Immm*, *a* = 0,93116(1) нм, *b* = 0,94993(1) нм, *c* = 0,98947(1) нм). Структурні розрахунки засвідчили відхилення від ідеальної стехіометрії 6:2:1, що відповідає формулі Dy<sub>6</sub>Ni<sub>2.43</sub>Sn<sub>0.5</sub>. Для сполуки встановлено послідовність магнітних фазових переходів; антиферомагнітне впорядкування виникає при 60 К, подальші магнітні фазові переходи порядок-порядок відбуваються за нижчих температур.

**Ключові слова:** Інтерметаліди; Кристалічна структура; Магнітні властивості; Питома теплоємність.